JOURNAL OF GUIDANCE, CONTROL, AND DYNAMICS
Vol. 24, No. 6, November–December 2001

Flight Mechanics of an Elastic Symmetric Missile

Charles H. Murphy and William H. Mermagen Sr.*
U.S. Army Research Laboratory, Aberdeen Proving Ground, Maryland 21156-0269

The free-flight motion of an elastic missile is approximated by three bodies connected by two massless elastic cantilever beams. If the mass distribution of the three bodies is 1–2–1, the frequency of the symmetric oscillation of the outer bodies is within 5% of the classical frequency of the oscillation of a free–free beam. A second combined pitching antisymmetric flexing motion can occur with a frequency that is almost twice that of the symmetric flexing motion. As the beam stiffness is reduced, the symmetric flexing motion frequency approaches the rigid-body aerodynamic zero-spin frequency, and the flight zero-spin aerodynamic frequency is considerably reduced. Moderate beam damping can cause dynamic instability for spins greater than the aerodynamic frequency. Resonance mode amplification can occur when the spin is equal to the aerodynamic frequency, but more important, also when the spin is equal to the two elastic flexing frequencies. Spin-yaw lock-in is shown to occur at the lower elastic frequency.

Nomenclature

d	=	projectile body diameter
EI	=	stiffness of beams
E_j	=	dimensionless complex lateral location of c.m. of body j with respect to projectile c.m.
(F_{xj}, F_{yj}, F_{zj})	=	aerodynamic force exerted on body j
$(\hat{F}_{xj}, \hat{F}_{yj}, \hat{F}_{zj})$	=	elastic beam force exerted on body j
g_1	=	$\rho V^2 S/2$
$\boldsymbol{H}_j$	=	angular momentum vector of body j
I_t	=	transverse moment of inertia of projectile
I_{tj}	=	transverse moment of inertia of body j
I_x	=	axial moment of inertia of projectile
I_{xj}	=	axial moment of inertia of body j
$I\{z\}$	=	imaginary part of z
L_j	=	dimensionless length of body j, that is, fineness ratio
(M_{xj}, M_{yj}, M_{zj})	=	aerodynamic moment exerted on body j
$(\hat{M}_{xj}, \hat{M}_{yj}, \hat{M}_{zj})$	=	elastic beam moment exerted on body j
m	=	projectile mass
m_j	=	mass of body j
p	=	projectile spin, p_1
p_j	=	axial component of angular velocity of body j
Q	=	complex angular velocity of body 1, $\dot{\theta} + i\dot{\psi}$
$R\{z\}$	=	real part of z
r_m	=	mass ratio, m_2/m
S	=	body cross-sectional area, $\pi d^2/4$
V	=	magnitude of projectile velocity
(v_{xj}, v_{yj}, v_{zj})	=	velocity of body j
(X_j, Y_j, Z_j)	=	location of c.m. of body j with respect to the c.m. of body 1
x_j	=	dimensionless axial location of c.m. of body j with respect to the c.m. of the projectile
α	=	angle of attack at the projectile c.m.
β	=	angle of sideslip at the projectile c.m.
$(\Gamma_{yj}, \Gamma_{zj})$	=	pitch and yaw angles of body j with respect to body 1
θ	=	pitch angle of body 1
λ_k	=	damping of kth mode
ξ	=	complex angle of attack of projectile, $\beta + i\alpha$
ρ	=	air density
σ	=	$\hat{\omega}/\omega_R$

Charles Murphy received his Ph.D. degree in Aeronautics from Johns Hopkins University in 1957. After spending many years in applied research at Aberdeen Proving Ground, MD, he retired from the Army Research Laboratory in 1997. He has published extensively in the field of missile flight mechanics and coauthored the book The Paris Guns and Project HARP. He has personally directed the firing of a sounding projectile to the record altitude of 111 miles above the Arizona desert from an extended 16-in. gun. He was the 1976 recipient of the AIAA Mechanics and Control of Flight Award, has received many Army awards, and is an AIAA Fellow.

William Mermagen is a retired federal executive and consultant to the information technology and aerospace industries. He was formerly Director of Corporate Information and Computing at the U.S. Army Research Laboratory. His research interests are in information sciences, ballistic sciences, and high-performance computing and communications. He has published and presented his personal research in more than 185 technical papers, conferences, and presentations. He holds a B.S. in physics from Fordham University and an M.S. in physics from the University of Delaware. He has been an Associate Fellow of the AIAA.

Received 15 May 2000; revision received 7 November 2000; accepted for publication 9 November 2000.

ϕ = roll angle of body 1
$\dot{\phi}_k$ = frequency of kth mode
ψ = yaw angle of body 1
$\hat{\omega}$ = $\sqrt{[3EI/(m_1 m_2 a^3)]}$
ω_R = rigid-projectile zero-spin frequency, $\sqrt{(T_{11}/I_t)}$
ω_1 = lowest frequency for free–free uniform elastic beam

Subscripts

B = parameter for bent projectile
e = Earth-fixed axes
R = parameter for rigid symmetric projectile

Superscripts

$\hat{}$ = quantity related to elastic beam
$\sim$ = aerodynamic quantity

I. Introduction

THE linear flight mechanics of spinning projectiles was first developed after World War I and later extended past World War II.[1–4] These results were reformulated by Platus[5] in missile-fixed coordinates for reentry vehicles. Thus, the linear flight mechanics of symmetric projectiles including finned missiles is well established. Nonlinear flight mechanics as well as the effect of liquid payloads have also been extensively addressed.[4,6,7]

Recently with the development of long finned antiarmor projectiles and long flare-stabilized reentry vehicles, the effects of aeroelasticity have become a matter of possible concern for designers. In 1992 Platus[8] developed a simple theory for elastically deforming missiles. This theory showed significant decreases in pitching frequency when the smallest bending frequency was less than four times the pitching frequency. He also showed that linear beam damping could actually make the missile dynamically unstable when the spin was greater than the pitching frequency.

Platus[8] assumed that the elastic missile oscillated in the modal waveform of a nonspinning free–free beam. For uniform distribution of mass, the waveform is symmetric with equal deflections at each end. The aerodynamic loads on a finned missile, however, are quite different at the nose and the tail, and this may not be a good assumption. Moreover, it would be desirable to predict the resonant response induced by mass or aerodynamic asymmetries at aerodynamic or elastic frequencies.

Murphy[9] has studied the response of a spin-stabilized body of revolution to the motion of an interior elastic beam-mounted mass and have shown that beam damping could destabilize the shell. Because all shells have spin rates in excess of their pitching frequencies, this is in agreement with the Platus result.[8]

In this paper, we will make use of beam theory[9] to construct a simple model of an elastic projectile acted on by two significant aerodynamic loads. The complicated elastic projectile will be replaced by three rigid-projectile components connected by two massless cantilevered beams. Next this three-body model will be used to yield good predictions of the frequency of the motion of a uniform free–free beam flying in a vacuum. With the inclusion of aerodynamic terms, frequencies and damping of the angular motion of a symmetric elastic missile can be estimated from a 5×5 determinant.

Beam damping should be based on derivatives in a missile-fixed coordinate system. Thus, beam damping has no effect on the trim motion, which is constant in these coordinates. Resonance frequencies, however, will decrease as the ratio of elastic frequency to rigid-body pitching frequency decreases. It will be shown that the damping of transients can be adversely affected by beam damping.

Finally, the effect of permanent deformations will be considered, that is, the case of a bent missile. These deformations affect the size of resonant trim and introduce the possibility of spin-pitch lock-in.[10]

II. Linearized Equations of Motion

We will initially consider a homogenous cylinder of fineness ratio L and mass m, divided into three segments with fineness ratios L_j and masses m_j. A fixed plane coordinate system that pitches and yaws with the center segment (component 1) and has an origin located at the c.m. of the center segment is shown in Figs. 1 and 2. (Fixed plane coordinates roll so that the Z axis is always in the $X_e - Z_e$ plane.) Its orientation with respect to Earth-fixed axes (ψ, θ) and the velocity vector (β, α) is also shown in Figs. 1 and 2.

For $j = 2$ and 3, let (X_j, Y_j, Z_j) be the location of the c.m. of component j with respect to the c.m. of component 1 and let $(\Gamma_{yj}, \Gamma_{zj})$ be the inclination of the forward body $(j = 2)$ and of the rear body $(j = 3)$, as shown in Figs. 1 and 2.

Next it is assumed that the fore and aft components are elastically connected to the center component by two massless cantilever beams of lengths a and b and stiffness EI. The moment and force exerted on these components by these beams can be computed from simple beam theory.[9] For motion in the $X-Y$ plane,

$$\hat{F}_{yj} = b_{1j} Y_j + b_{2j} \Gamma_{yj} \tag{1}$$

$$\hat{M}_{zj} = b_{2j} Y_j + b_{3j} \Gamma_{yj} \tag{2}$$

where

$$b_{12} = -(12/a^3)(EI), \qquad b_{13} = -(12/b^3)(EI)$$
$$b_{22} = (6/a^2)(EI), \qquad b_{23} = -(6/b^2)(EI)$$
$$b_{32} = -(4/a)(EI), \qquad b_{33} = -(4/b)(EI)$$

Similar relations apply for $\hat{F}_{zj}$ and $\hat{M}_{yj}$.

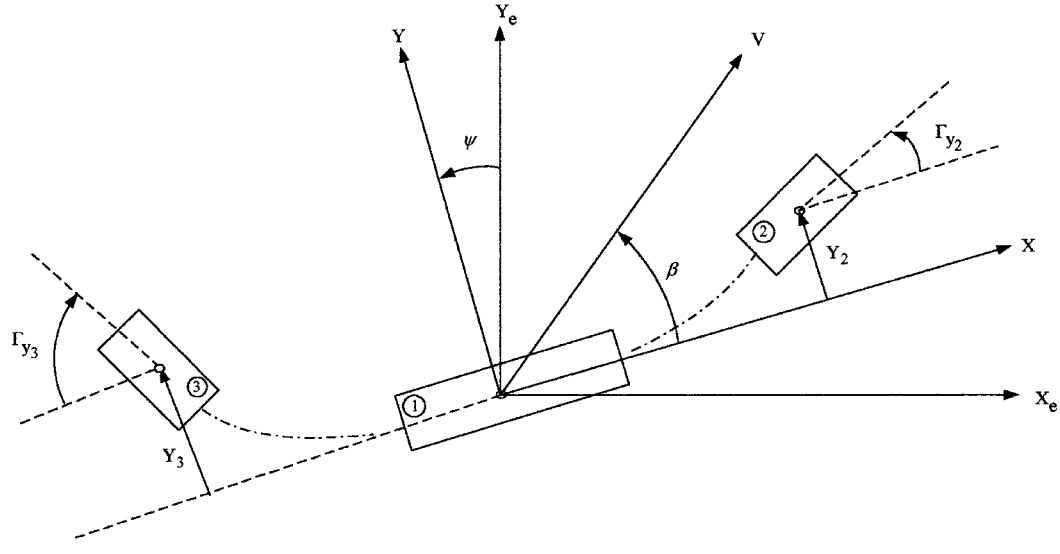

Fig. 1 X–Y coordinates for three-component projectile (every variable is shown as positive except Γ_{y3}).

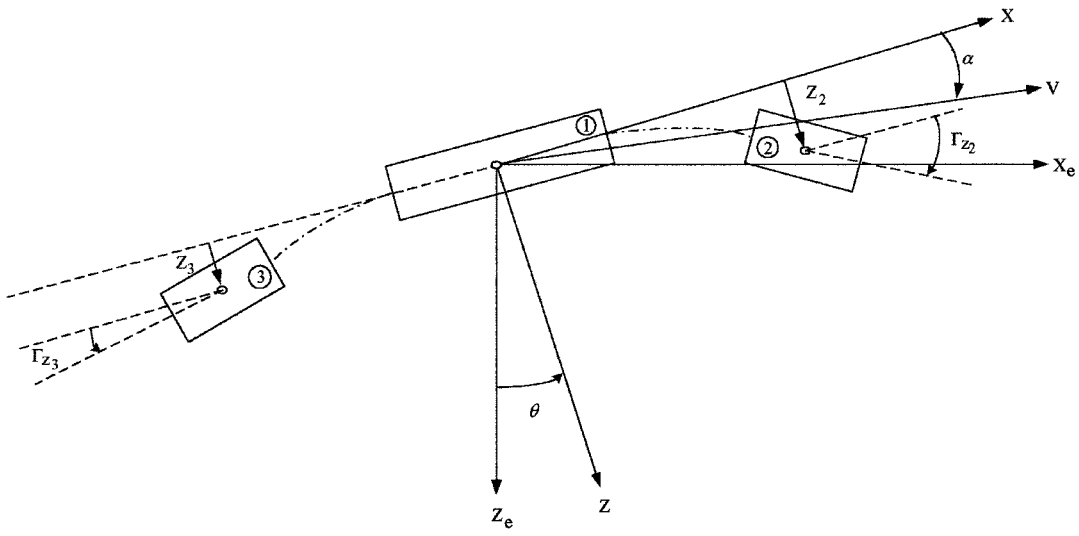

Fig. 2 X–Z coordinates for three-component projectile (every variable is shown as positive except Γ_{z3}).

For the dynamics analysis, a coordinate system with its origin at the c.m. of the complete projectile is much more convenient. Throughout this paper, complex quantities will be used to describe the lateral motion of the three components. Their lateral location will be specified by the dimensionless complex variables E_j and their axial location by dimensionless variable x_j. Both the lateral locations and the axial locations are with respect to the projectile c.m.:

$$E_j - E_1 = (Y_j + iZ_j)/d, \qquad E_1 = -(m_2E_2 + m_3E_3)/m_1 \quad (3)$$

$$x_j = (X_j/d) + x_1, \qquad x_1 = -(m_2X_2 + m_3X_3)/md \quad (4)$$

The complex beam forces and moments exerted on the forward and aft components are

$$\hat{F}_j = b_{1j}(E_j - E_1)d + b_{2j}\Gamma_j \quad (5)$$

$$\hat{M}_j = i[b_{2j}(E_j - E_1)d + b_{3j}\Gamma_j] \quad (6)$$

where

$$\Gamma_j = \Gamma_{yj} + i\Gamma_{zj}$$

The velocity vector of the j component is (v_{xj}, v_{yj}, v_{zi}), and the complex transverse velocity is

$$v_{yj} + iv_{zj} = \dot{E}_j d + V\xi - ix_j Qd \quad (7)$$

where $\xi = \beta + i\alpha$ is the complex angle of attack, $Q = \dot{\theta} + i\dot{\psi}$ is the complex transverse angular velocity, and $V \cong v_{xj}$ is the magnitude of the projectile's velocity.

The transverse components of the equations of motion for each component's c.m. can provide differential equations for the E_j:

$$m_j[\ddot{E}_j d + V(\dot{\xi} - iQ) + \dot{V}\xi - ix_j\dot{Q}d] = \hat{F}_j + F_j \quad (8)$$

where F_j is the transverse aerodynamic force acting on the j component. The axial beam forces $\hat{F}_{xj}$ are determined by the requirement that each component has the same axial velocity,

$$m_j\dot{V} \cong m_j v_{xj} = \hat{F}_{xj} + F_{xj} \quad (9)$$

where F_{xj} is the axial aerodynamic force acting on the j component.

The angular momentum of each component $\boldsymbol{H}_j$ can be simply expressed in fixed plane coordinates that pitch and yaw with that component:

$$\boldsymbol{H}_j = [I_{xj}p,\ I_{tj}(\dot{\theta} - \dot{\Gamma}_{zj}),\ I_{tj}(\dot{\psi} + \dot{\Gamma}_{yj})] \quad (10)$$

where $\Gamma_1 = 0$. After differentiating each angular momentum vector, we can write three differential equations for the two Γ_j and Q from the transverse components,

$$I_{tj}(\dot{Q} + i\ddot{\Gamma}_j) - ipI_{xj}(Q + i\dot{\Gamma}_j) = \hat{M}_j + M_j \quad (11)$$

where M_j is the transverse aerodynamic moment acting on the j component.

The forces exerted on the center component by the other components are the negatives of the beam forces and the moment exerted on the center component can be computed from the negatives of the beam forces and moments:

$$\hat{F}_1 = -\hat{F}_2 - \hat{F}_3, \qquad \hat{F}_{x1} = -\hat{F}_{x2} - \hat{F}_{x3} \quad (12)$$

$$\hat{M}_1 = -\hat{M}_2 - \hat{M}_3 - i[(x_2 - x_1)\hat{F}_2 + (x_3 - x_1)\hat{F}_3 + \hat{F}_{x2}(E_2 - E_1) + \hat{F}_{x3}(E_3 - E_1)]d \quad (13)$$

The sum of Eq. (9) yields the usual drag equation,

$$m\dot{V} = \sum_{j=1}^{3} F_{xj} \quad (14)$$

Equation (8) can be added to eliminate the beam forces to provide a simple relation between Q and ξ:

$$V(\dot{\xi} - iQ) = \sum_{j=1}^{3}[F_j - \xi F_{xj}] \quad (15)$$

Equation (8) can now be multiplied by $i(x_j - x_1)d$, respectively, Eq. (9) multiplied by $i(E_j - E_1)d$, and all added to the sum of Eq. (11) to eliminate the beam forces and moments. The resulting differential equation for Q can then be simplified to

$$I_t\ddot{Q} - ipI_xQ = \sum_{j=2}^{3}\left[m_j(x_j - x_1)\ddot{E}_j d^2 + I_{tj}\ddot{\Gamma}_j - ipI_{xj}\dot{\Gamma}_j\right] + \sum_{j=1}^{3}[M_j + i(x_jF_j + F_{xj}E_j)d] \quad (16)$$

where

$$I_t = I_{t1} + I_{t2} + I_{t3} + \left(m_1x_1^2 + m_2x_2^2 + m_3x_3^2\right)d^2$$

$$I_x = I_{x1} + I_{x2} + I_{x3}$$

III. Linear Aerodynamics

The linear aerodynamic forces and moments acting on the three bodies have the following forms in terms of the angle of attack at each body:

$$F_{xj} = -g_1 c_{Dj}, \qquad g_1 = \rho V^2 S/2 \tag{17}$$

$$F_{yj} + iF_{zj} = -g_1\left\{\left[c_{1j} + i(pd/V)c^*_{1j}\right]\xi_j + c_{2j}\dot{\xi}_j d/V\right\} \tag{18}$$

$$M_{yj} + iM_{zj} = -ig_1 d\left\{\left[c_{3j} + i\left(pd/V\right)c^*_{3j}\right]\xi_j + c_{4j}\dot{\xi}_j d/V\right\} \tag{19}$$

The Magnus force and moment coefficients c^*_{1j} and c^*_{3j} are usually neglected for slowly spinning finned missiles but must be retained for spin-stabilized bodies of revolution. The local angles of attack at the three components are determined by their location, inclinations, and motion

$$\xi_j = \xi - \dot{\xi}x_j d/V - \Gamma_j + \dot{E}_j d/V \tag{20}$$

[Note that in Ref. 8 the relation similar to Eq. (20) erroneously uses the missile-fixed derivative of E_j and not the derivative in a nonspinning coordinate system.]

From Eqs. (14) and (17), the familiar form of the drag equation can be written:

$$m\dot{V} = -g_1 C_D \tag{21}$$

where

$$C_D = c_{D1} + c_{D2} + c_{D3}$$

Equations (17) and (18) for the aerodynamic force can be inserted in Eq. (14) and the small effects of the Magnus force, the damping force, and the centerbody lift on the trajectory neglected:

$$(c^*_{1j} = c_{2j} = c_{11} = 0)$$

$$mV(\dot{\xi} - iQ) = -g_1\lfloor C_{L\alpha}\xi - c_{12}(\Gamma_2 - \dot{E}_2 d/V) - c_{13}(\Gamma_3 - \dot{E}_3 d/V)\rfloor \tag{22}$$

where

$$C_{L_\alpha} = C_{N\alpha} - C_D$$

Equations (8) and (11) for $j = 2, 3$ and Eqs. (15) and (16) are six differential equations in six variables, ξ, Q, E_2, Γ_2, E_3, and Γ_3. If the aerodynamic forces and moments of Eqs. (17–19) are inserted and Q eliminated by use of Eq. (22), a set of five equations in five variables results:

$$\sum_{m=1}^{5}\left[R_{nm}\ddot{z}_m + \left(S_{nm} + ipS^*_{nm}\right)\dot{z}_m + \left(T_{nm} + ipT^*_{nm}\right)z_m\right] = 0 \qquad n = 1, 2, 3, 4, 5 \tag{23}$$

where

$$(z_1, z_2, z_3.z_4, z_5) = (\xi, E_2, \Gamma_2, E_3, \Gamma_3)$$

R_{nm} and S^*_{nm} are primarily dynamics terms involving various masses and moments of inertia. The aerodynamic contributions to these terms are quite small and will be neglected. T_{nm} contains combinations of beam elastic terms and aerodynamic terms whereas S_{nm} and T^*_{nm} are combinations of beam damping terms and aerodynamic terms:

$$T_{nm} = \hat{T}_{nm} + g_1\tilde{T}_{nm}, \qquad S_{nm} = \hat{S}_{nm} + (g_1 d/V)\tilde{S}_{nm}$$

$$T^*_{nm} = \hat{T}^*_{nm} + (g_1 d/V)\,\tilde{T}^*_{nm} \tag{24}$$

Of the 40 terms, 20 of the dynamics terms, 12 of the elastic terms, and 8 of the beam damping terms are nonzero. These 40 terms and the 46 nonzero aerodynamic terms are tabulated in Ref. 11.

A general solution of Eq. (23) can be expressed as a linear combination of 10 modal functions of the form

$$z_m = z_{mk}\, e^{At}, \qquad A = A_k, \qquad k = 1{-}10 \tag{25}$$

When a function of this type is substituted into Eq. (23), the final result can be written in the form of five linear homogenous equations in the constants z_{mk}. These equations are specified by a 5×5 matrix u_{nm}, which is a function of A:

$$\sum_{m=1}^{5} u_{nm} z_{mk} = 0, \qquad n = 1, 2, 3, 4, 5 \tag{26}$$

where

$$u_{nm} = A_k^2 R_{nm} + A_k\left(S_{nm} + ipS^*_{nm}\right) + T_{nm} + ipT^*_{nm}$$

The 10 values of A_k are the roots of

$$\det u_{nm} = 0 \tag{27}$$

For $z_{1k} \neq 0$, the corresponding values of the z_{mk} for each of the 10 modes can be determined from the solution of a fourth-order inhomogeneous linear system:

$$\sum_{m=1}^{4} w_{nm} y_{mk} = w_n, \qquad n = 1, 2, 3, 4 \tag{28}$$

where

$$w_{nm} = u_{(n+1)(m+1)}, \qquad y_{mk} = z_{(m+1)k}/z_{1k}, \qquad w_n = -u_{(n+1)1}$$

Equation (27) can be solved in general by a simple trial and error Newton's method.

IV. Three-Component Motion in a Vacuum

We will consider a nonspinning projectile with identical components 2 and 3 and identical connecting beams. For this case, all parameters for components 2 and 3 are equal except for $x_2 = -x_3$ and $b_{22} = -b_{23}$. For motion in a vacuum, $g_1 = 0$, and the aerodynamic terms vanish. The resulting equations identify zero as a double root of Eq. (27) ($A_1 = A_2 = 0$). If we consider symmetric flexing motion for which $z_{2k} = z_{4k}$ and $z_{3k} = -z_{5k}$, the pitching motion described by z_{1k} has zero amplitude. Four more roots of Eq. (27) follow.

For small I_{t2},

$$A_{3,4} = \pm i\sqrt{\frac{3mEI}{m_1 m_2 a^3}} = \pm i\hat{\omega}$$

$$A_{7,8} = \pm 2i\sqrt{\frac{EI}{I_{t2}a}} \tag{29}$$

The third and fourth roots are particularly interesting because they produce flexing motion similar to that for the classical free–free beam vibration. The lowest frequency for this motion as given by Ref. 12 is

$$\omega_1 = 22.37\sqrt{EI/(mL^3d^3)} \tag{30}$$

If we assume the length of the beam to be the distance between the c.m. of the center component and the forward component,

$$a = x_2 d = \frac{(L/2)(1 + r_m)}{(1 + 2r_m)} \tag{31}$$

$$\frac{\omega_1}{\hat{\omega}} = (4.566)\sqrt{\frac{r_m(1 + r_m)^3}{(1 + 2r_m)^5}} \tag{32}$$

where

$$r_m = m_2/m_1$$

According to Eq. (32), the three-body frequency is only 5% greater than the classical frequency when the masses for fore and aft components each are one-half the mass of the center component or are each 25% of the total mass. In the numerical examples of this report, we will specify each end component to have one-quarter the total mass.

The remaining four roots can be obtained by assuming an antisymmetric oscillation of the end bodies, that is, $z_{2k} = -z_{4k}$ and $z_{3k} = z_{5k}$. The amplitude of the pitching motion is coupled to the amplitude of the flexing motion by

$$z_{1k} = 2\left\lfloor m_2 x_2 d^2 z_{2k} + I_{t2} z_{3k} \right\rfloor / I_t \tag{33}$$

For small I_{t2},

$$A_{5,6} = \pm i\sqrt{\frac{3EI}{m_2 a_1 a^3}}, \qquad A_{9.10} = \pm 2i\sqrt{\frac{EI}{I_{t2} a}} \tag{34}$$

where

$$a_1 = 1 - 2m_2(x_2)^2 d^2 / I_t$$

The 9 and 10 roots are approximately equal to the 7 and 8th roots. These roots correspond to very high frequencies and will not be considered in the remainder of this paper.

V. Flare-Stabilized Rod

Platus[8] first applied his theory to a 5-ft-long rod stabilized by a very light 1.5-ft-long flare with a base diameter of 0.8 ft. Because he neglected the very small normal force associated with the nose, this missile has a very simple normal force distribution:

$$\frac{dC_{N\alpha}}{dx} = -1.138(x + 1.25), \qquad -3.12 \le x \le -1.25 \tag{35}$$

The ratio of the three-body elastic frequency $\hat{\omega}$ to the rigid-body zero-spin pitch frequency ω_R is a good measure of the effect of elasticity on the projectile's aerodynamic frequencies and damping rates. This ratio, $\hat{\omega}/\omega_R$, will be denoted by σ and is usually greater than 5. When it is less than 5, we would expect a large effect on the aerodynamic motion. By varying EI, we can compute $\dot{\phi}_1/\omega_R$ as a function of σ. The result is plotted as Fig. 3 and compared with the three-body theory. Figure 3 show similar behavior for the two theories, but the three-body theory predicts a much slower decrease in $\dot{\phi}_1$ with decreasing σ. The displacement of the aft component is twice that of the forward component. For $\sigma = 2$, the fin angle of attack is reduced by 40%, thereby reducing the frequency by 23%.

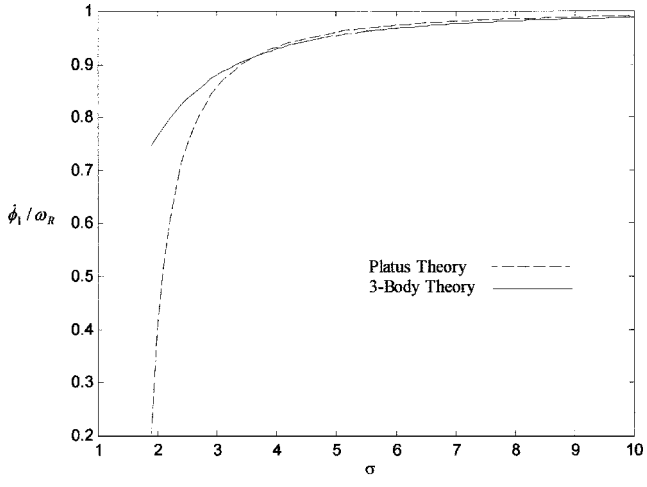

Fig. 3 For flare stabilized rod, $\dot{\phi}_1/\omega_R$ vs σ.

VI. Finned Missile

The implications of our aeroelastic theory can best be seen by the consideration of a particular hypersonic finned projectile with fineness ratio of 20 flying at 6000 ft/s. This projectile has a body diameter of 0.35 ft, and its forward and rear segments are each 25% of the total length. The various aerodynamic coefficients are computed from an assumed force distribution. This force distribution was obtained from slender body theory[13] for the body alone and from linearized supersonic theory for the four fins.[14] All parameters are listed in Table 1 and the missile shown in Fig. 4. For zero spin, the rigid-body frequency ω_R is 8.52 Hz and rigid-body damping rate is $-2.4\ s^{-1}$. For $\sigma = 8$, the three-body symmetric beam frequency ω is 69.0 Hz, and the elastic projectile frequency is 8.06 Hz, that is, 6.5% less than the rigid-body frequency.

The equations derived in Sec. III can now be used to calculate $\dot{\phi}_1/\omega_R$ as a function of σ between 1.0 and 10.0, and the result is shown in Fig. 5. For $\sigma = 4$, the effective angle of attack of the fins has been reduced by 30%, and the adverse angle of the nose has increased by 35%, thereby reducing the projectile frequency by 45%. The large nose deflection with its increased destabilizing moment has a large effect on the projectile frequency, which did not appear for the flare-stabilized missile.

VII. Beam Damping

Beam damping is a very complicated process that we will approximate by a simple linear proportionality with the displacement velocity. This velocity must be computed in a coordinate system

Table 1 Finned missile parameters

Parameter	Value	Parameter	Value
m	3.50 slug	c_{D3}	0.18
$m_2 = m_3$	0.875 slug	c_1	9.4
I_x	0.054 slug · ft^2	c_3	−34.4
$I_{x2} = I_{x3}$	0.0135 slug · ft^2	c_4	−750
I_t	14.20 slug · ft^2	c_{12}	2.3
$I_{t2} = I_{t3}$	0.22 slug · ft^2	c_{13}	7.1
$x_2 = -x_3$	7.5 cal	c_{22}	19
$(EI)_2$	$(EI)_3$	c_{23}	27
d	0.35 ft	c_{32}	5.4
$a = b$	2.63 ft	c_{33}	−3.6
ρ	0.002 slug/ft^3	c_{42}	−30
V	6000 ft/s	c_{43}	−10
C_D	0.40	$C_{\ell p}$	−18
c_{D2}	0.15	All other	$c_j 0$

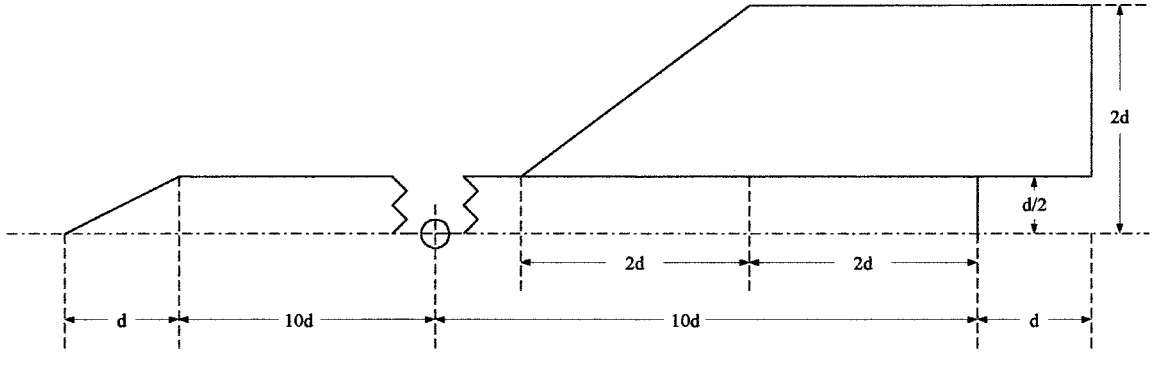

Fig. 4 Finned missile.

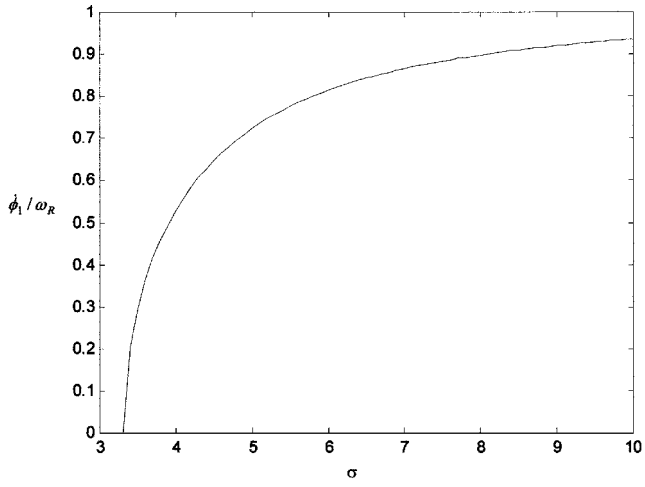

Fig. 5 For finned missile, $\dot{\phi}_1/\omega_R$ vs σ.

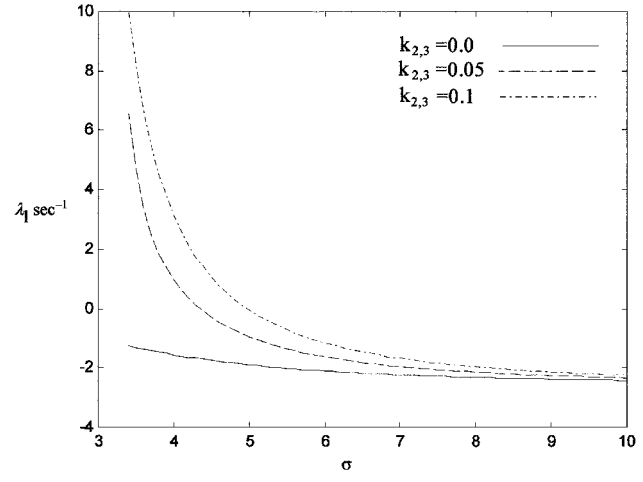

Fig. 6 For $p = 2.3\,\omega_R$, λ_1 vs σ, where $k_2 = k_3 = 0$, 0.05, and 0.10.

spinning with the beam. Thus, the damping force exerted by each beam is assumed to have the form

$$\left(\hat{F}_{yj} + i\hat{F}_{zj}\right)_{\text{damp}} = -2k_j m_j \hat{\omega} e^{i\phi} \frac{\mathrm{d}}{\mathrm{d}t}\left[(E_j - E_1)e^{-i\phi}\right]$$
$$= -2k_j m_j \hat{\omega}[\dot{E}_j - \dot{E}_1 - ip(E_j - E_1)] \quad (36)$$

where

$$\dot{\phi} = p$$

The definition of k_j was selected so that $k_j = 1$ corresponds to critical damping of a free–free beam. The forward beam damping contribution to the first mode is, for example,

$$-2k_2 m_2 \hat{\omega}\lfloor \lambda_1 + i(\dot{\phi}_1 - p)\rfloor[(m_1 + m_2)z_{21} + m_3 z_{41}]/m_1$$

Thus, beam damping is a strong function of spin and is essentially zero when spin is equal to the modal frequency. Beam damping increases projectile damping when spin is less the modal frequency and decreases projectile damping when it is greater than modal frequency. Finally, Fig. 6 shows λ_1 vs σ for spin of $2.3\omega_R$ and $k_2 = k_3 = 0$, 0.05, and 0.10. For low values of σ, beam damping actually can cause projectile instability.

VIII. Bent Missile

If the beam deflection is large enough, the maximum stress exceeds the yield limit, and the beams are permanently deformed or bent. All future elastic motion will be about this new bent shape. Thus, the component location variables E_j and Γ_j are no longer completely elastic, but consist of an elastic part and a permanently bent part that rotates with the projectile:

$$E_j = \hat{E}_j + E_{jB}e^{i\phi} \quad (37)$$

$$\Gamma_j = \hat{\Gamma}_j + \Gamma_{jB}e^{i\phi} \quad (38)$$

where $\dot{\phi} = p$ and $\hat{E}_j$ and $\hat{\Gamma}_j$ vary elastically. Both fore and aft components will have trim force and trim moment terms associated with Γ_{jB} and E_{jB} in Eq. (20).

The equations of motion derived in Sec. 3 should be modified by inserting the new variables of Eqs. (37) and (38) in the dynamics and aerodynamics terms and replacing (E_j, Γ_j) by $(\hat{E}_j, \hat{\Gamma}_j)$ in the elastic terms. Our new set of five inhomogeneous differential equations contains terms multiplied by $\exp(i\phi)$:

$$\sum_{m=1}^{5}\left[R_{nm}\ddot{z}_m + \left(S_{nm} + ipS^*_{nm}\right)\dot{z}_m + \left(T_{nm} + ipT^*_{nm}\right)z_m\right] = t_n \exp(i\phi)$$
$$n = 1, 2, 3, 4, 5 \quad (39)$$

where t_n are tabulated in Ref. 11.

We assume constant spin and a solution of the form

$$(z_1, z_2 \cdot z_3, z_4, z_5) = (\xi_T, \hat{E}_{2T} \cdot \hat{\Gamma}_{2T}, \hat{E}_{3T}, \hat{\Gamma}_{3T})\exp(ipt)$$
$$= (s_1, s_2, s_3, s_4, s_5)\exp(ipt) \quad (40)$$

The s_j are solutions of the following linear inhomogeneous system of equations:

$$\sum_{m=1}^{5} t_{nm}s_m = t_n, \qquad n = 1, 2, 3, 4, 5 \quad (41)$$

where

$$t_{nm} = -p^2\left(R_{nm} + S^*_{nm}\right) + ip\left(S_{nm} + T^*_{nm}\right) + T_{nm}$$

We will consider a simple bent version of our finned missile. All of the bent parameters are taken to be zero except for $E_{3B} = -0.063$ and $\Gamma_{3B} = 0.020$. The magnitude of the trim motion is smaller than that for zero-spin motion except in the vicinity of the five resonant spins. For $\sigma = 5$, the maximum values of the trim motion parameters for spin near the three lower resonant frequencies are given in Table 2 and s_1/s_{10} vs spin is shown in Fig. 7.

Table 2 Resonant spins s_j/s_{10}, $\sigma = 5$

p	$0.74\,\omega_R$	$4.87\,\omega_R$	$9.72\,\omega_R$
s_1/s_{10}	10.0 (−87)	1.2 (106)	10.9 (−104)
s_2/s_{10}	4.9 (93)	22.1 (103)	90 (−104)
s_3/s_{10}	2.2 (93)	8.8 (102)	19.5 (−104)
s_4/s_{10}	4.7 (92)	16.2 (102)	93.3 (76)
s_5/s_{10}	2.0 (−88)	7.3 (−78)	20.6 (−105)

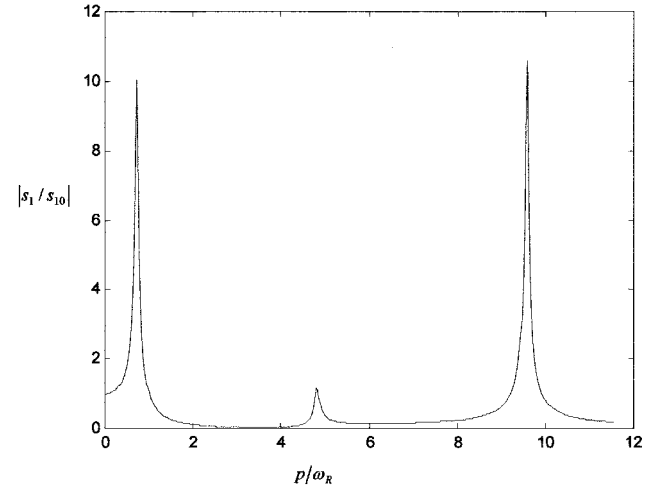

Fig. 7 For $\sigma = 5$, $|s_1/s_{10}|$ vs p/ω_R

For spin near $0.7\omega_R$ and $4.9\omega_R$, the forward and aft components move in phase with each other while they are out of phase for spin near $9.7\omega_R$. This out of phase motion is similar to the fifth and sixth modes for vacuum flight. For resonant spins of $0.7\omega_R$ and $9.7\omega_R$, the aft component moves to reduce the effective angle of attack of the fins, but it actually increases the effective angle of attack for the intermediate spin of $4.9\omega_R$. The motion of the two end bodies does dominate the two elastic beam resonant frequencies.

IX. Quadratic Roll Equation

Because the trim motion is large in a very small region near resonant spin, trim motion of rigid spinning finned missiles is usually a minor concern for designers. Some missiles, however, can lock-in at resonant spin for a range of initial conditions. In Ref. 10, it is shown that a rigid missile with mass asymmetry and a trim aerodynamic force can lock-in at resonant spin. The terms in the missile's roll equation that causes this are quadratic terms, and we must, therefore, derive the quadratic version of roll equations for the three components.

Each component's roll equation is expressed with respect to that component's fixed plane X axis:

$$I_{xj}\dot{p}_j = \hat{M}_{xj} + g_1 c_{\ell j} d \tag{42}$$

If linearity is assumed,

$$p_1 = p_2 = p_3 = p \tag{43}$$

$$\hat{M}_{x1} = -\hat{M}_{x2} - \hat{M}_{x3} \tag{44}$$

$$I_x \dot{p} = g_1 c_\ell d \tag{45}$$

where

$$c_\ell = c_{\ell 1} + c_{\ell 2} + c_{\ell 3} = C_{\ell p}\,(p - p_{ss})\,d/V$$

where p_{ss} is the linear steady-state spin produced by either intentional cant of the fins or unintentional damage to the fins.

The exact relations for p_2 and p_3 depend on the requirement that they should be equal to the corresponding body's fixed plane X component of the central body's angular velocity:

$$\begin{aligned} p_j &= p\left[\left(1-\gamma_j^2\right)/2\right] + \dot{\theta}\Gamma_{yj} + \dot{\psi}\Gamma_{zj} \\ &= p + R\{(Q - p\Gamma_j/2)\bar{\Gamma}_j\} \end{aligned} \tag{46}$$

where

$$\gamma_j = |\Gamma_j|, \qquad R\{a+ib\} = a$$

and $\bar{z}$ is the complex conjugate of z. Equation (44) can be replaced by a more exact expression for the roll moment exerted on the central body by the two beams as

$$\begin{aligned} \hat{M}_{x1} = &-\hat{M}_{x2}\left[1-\gamma_2^2/2\right] + R\{\hat{M}_2\bar{\Gamma}_2\} - \hat{M}_{x3}\left[1-\gamma_3^2/2\right] \\ &+ R\{\hat{M}_3\bar{\Gamma}_3\} - I\{\hat{F}_2(\bar{E}_2 - \bar{E}_1)d + \hat{F}_3(\bar{E}_3 - \bar{E}_1)d\} \end{aligned} \tag{47}$$

Equations (42), (46) and (47) can be combined to give the nonlinear version of Eq. (45):

$$\begin{aligned} \left[I_x - \left(I_{x2}\gamma_2^2 + I_{x3}\gamma_3^2\right)/2\right]\dot{p} = &\, g_1 c_\ell d + R\{\hat{M}_2\bar{\Gamma}_2 + \hat{M}_3\bar{\Gamma}_3\} \\ &- I\{\hat{F}_2(\bar{E}_2 - \bar{E}_1)d + \hat{F}_3(\bar{E}_3 - \bar{E}_1)d\} - \dot{C}_0 \end{aligned} \tag{48}$$

where

$$C_0 = \sum_2^3 I_{xj} R\left(\frac{Q - p\Gamma_j}{2}\right)\bar{\Gamma}_j$$

Equation (48) is the nonlinear spin equation and must be combined with Eq. (39) to describe the motion of a bent missile. Any study of the steady-state solutions would require numerical integration of Eqs. (39) and (48). The linear spin equation had a constant steady-state solution, and constant steady-state solutions for the nonlinear spin equation are possible. For constant spin, the trim motion given by Eqs. (40) and (41) describes the steady-state transverse motion of an elastic missile. If the equations for trim motion are inserted in Eq. (48) and $\dot{p}$ is taken to be zero, the appropriate equation for equilibrium spins can be written:

$$g_1 C_{\ell p}(p - p_{ss})\,d^2/V = -(M_x)_{nl} \tag{49}$$

where

$$\begin{aligned} (M_x)_{nl} = &\, R\{\hat{M}_{2T}\bar{\Gamma}_{2T} + \hat{M}_{3T}\bar{\Gamma}_{3T}\} - I\{\hat{F}_{2T}(\bar{E}_{2T} - \bar{E}_{1T})d \\ &+ \hat{F}_{3T}(\bar{E}_{3T} - \bar{E}_{1T})d\} \end{aligned}$$

if two functions of spin, $f_1\,(p)$ and $f_2\,(p)$, are defined as

$$f_1\,(p) = -(M_x)_{nl}\left(g_1 C_{\ell p} d^2/V\right)^{-1} \tag{50}$$

$$f_2\,(p) = p - p_{ss} \tag{51}$$

Equation (49) states that equilibrium spins are spins for which f_1 intersects f_1. Here $f_1\,(p)$ is a function of spin, and except for near resonance spin, it is quite small and equilibrium spin must be near the design p_{ss}. Near resonance, however, $f_1(p)$ is large. Although p_{ss} could be quite far from resonance spin, a near resonance spin could satisfy Eq. (49) and be an equilibrium spin. If this equilibrium spin were a stable equilibrium, it would be a possible constant steady-state spin and, therefore, produce spin-yaw lock-in. Numerical integration of the differential equations of motion, Eqs. (39) and (48), would determine the stability of the equilibrium spins.

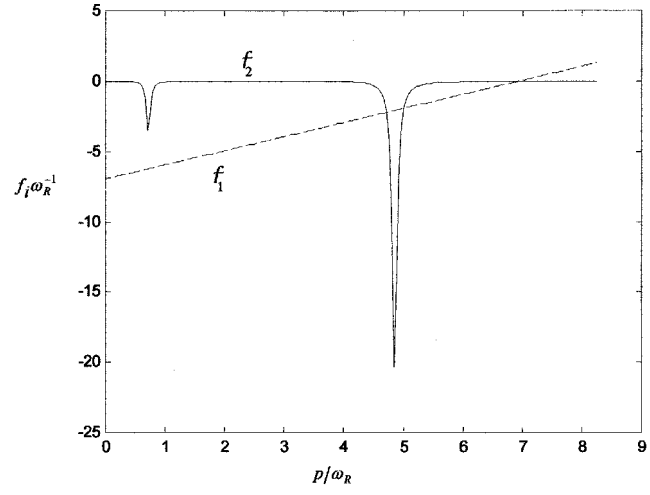

Fig. 8 For bent missile with $\sigma = 5$, $i = 1, 2$, $f_i\omega_R^{-1}$ vs p/ω_R.

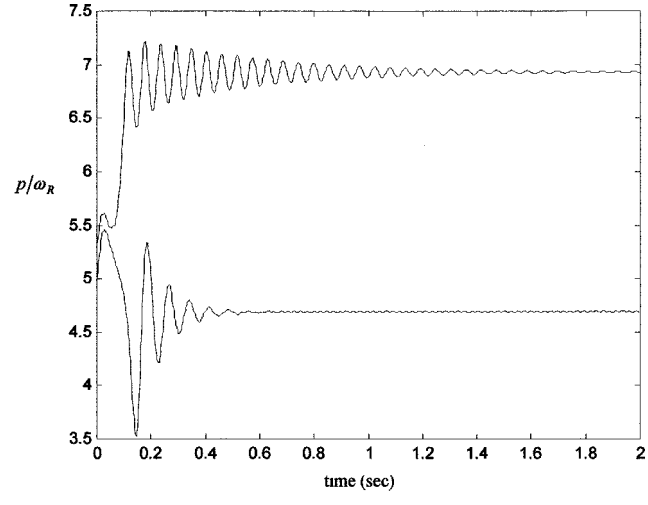

Fig. 9 For bent missile with $\sigma = 5$, p/ω_R vs time ($p_{ss} = 7\omega_R, \dot{p}_0 = 4.9\omega_R$, and $5.2\omega_R$).

Function $f_1(p)$ for a nonlinear roll moment is computed from Eq. (50) for our bent missile, and the result is plotted against p/ω_R in Fig. 8. The line $f_2(p)$ for the linear roll moment is also plotted for $p_{ss} = 7\omega_R$. The three intersections of the two curves are equilibrium spins. The effect of other values of p_{ss} can be determined by changing the p/ω_R intercept of the $f_2(p)$ line. This process shows that $0.7\omega_R$ could be an equilibrium spin when p_{ss} is between $0.7\omega_R$ and $3.1\omega_R$ and similar observations apply for $4.9\omega_R$.

The equations of motion for our bent missile case have been integrated for $p_{ss} = 7\omega_R$ and $\dot{p}_0 = 4.9\omega_R$, and $5.2\omega_R$. The resulting spin history is plotted against time in Fig. 9. For $\dot{p}_0$ greater than $5.2\omega_R$, the spin goes to a constant value near the linear prediction of p_{ss}. For $\dot{p}_0$ between 0 and $4.9\omega_R$, it goes to a value of $4.7\omega_R$ near the lowest elastic frequency. Thus, spin lock-in can occur for this elastic frequency.

X. Summary

1) Aeroelastic motion of a flexible projectile is approximated by three bodies connected by two massless elastic beams.

2) This three-component projectile theory gives excellent estimates of the first elastic frequency of a free–free uniform beam.

3) Two types of beam motion are simulated: the classical free–free symmetric motion and an outof-phase antisymmetric flexing motion combined with pitching motion.

4) When the elastic frequency is less than eight times the aerodynamic rigid-body pitch frequency, the fins move to reduce the stabilizing moment significantly and the pitch frequency can be significantly reduced.

5) Moderate beam damping can cause dynamic instability when the spin is much greater than the pitch frequency.

6) The trim motion of a bent missile shows large resonant responses when the spin is near the lower three modal frequencies.

7) The quadratic roll equation shows that lock-in can occur for the lower elastic frequency.

References[‡]

[1]Fowler, R. H., Gallop, J. L., Lock, C. N. H., and Richmond, H. W., "Aerodynamics of a Spinning Shell," *Philosophical Transactions of the Royal Society of London, Series A: Mathmatical and Physical Sciences*, Vol. 221, 1920, pp. 295–387.

[2]McShane, E. J., Kelley, J. L., and Reno, F., *Exterior Ballistics*, Univ. of Denver Press, Denver, CO, 1953.

[3]Nicolaides, J. D., "On the Free Flight Motion of Missiles Having Slight Configurational Asymmetries," U.S. Army Ballistic Research Lab., Rept. 858, Aberdeen Proving Ground, MD, June 1953; also Inst. of Aeronautical Sciences, Preprint 395, Jan. 1953.

[4]Murphy, C. H., "Free Flight Motion of Symmetric Missiles," U.S. Army Ballistic Research Lab., Rept. 1216, AD 442757, Aberdeen Proving Ground, MD, July 1963.

[5]Platus, D. H., "Ballistic Re-Entry Vehicle Flight Dynamics," *Journal of Guidance and Control*, Vol. 5, No. 1, 1982, pp. 4–16.

[6]Murphy, C. H., "Symmetric Missile Dynamic Instabilities," *Journal of Guidance and Control*, Vol. 4, No. 1, 1981, pp. 464–471.

[7]Murphy, C. H., Bradley, J. W., and Mermagen, W. H., "Side Moment Exerted by a Spinning, Coning, Highly Viscous Liquid Payload," U.S. Army Ballistic Research Lab., Rept. 3074, AD 218746, Aberdeen Proving Ground, MD, Dec. 1989.

[8]Platus, D. H., "Aeroelastic Stability of Slender, Spinning Missiles," *Journal of Guidance, Control, and Dynamics*, Vol. 15, No. 1, 1992, pp. 144–151.

[9]Murphy, C. H., "Spinning Projectile Instability Induced by an Internal Mass Mounted on an Elastic Beam," U.S. Army Research Lab., Rept. MR 270, AD 302047, Aberdeen Proving Ground, MD, Nov. 1995; also AIAA Paper 92-4493-CP, Aug. 1992.

[10]Murphy, C. H., "Some Special Cases of Spin-Yaw Lock-In," *Journal of Guidance, Control, and Dynamics*, Vol. 12, No. 6, 1989, pp. 771–776; also U.S. Army Research Lab., Rept. BRL MR 3609, AD A185295, Aberdeen Proving Ground, MD, Aug. 1987.

[11]Murphy, C. H., and Mermagen, W. H., "Flight Mechanics of an Elastic Symmetric Missile," U.S. Army Research Lab., Rept. TR-2255, Aberdeen Proving Ground, MD, Jan. 2001.

[12]Geradin, M., and Rixen, D., *Mechanical Vibrations*, Wiley, New York, 1997.

[13]Wood, R. M., and Murphy, C. H., "Aerodynamic Derivatives of Both Steady and Nonsteady Motion of Slender Bodies," *Journal of the Aeronautical Sciences*, Vol. 22, Dec. 1955, pp. 870–71; also U.S. Army Research Lab., Rept. BRL MR 880, AD 66178, Aberdeen Proving Ground, MD, April 1055.

[14]Boltz, R. E., and Nicolaides, J. D., "A Method of Determining Some Aerodynamic Coefficients from Supersonic Free Flight Tests of a Rolling Missile," *Journal of the Aeronautical Sciences*, Vol. 17, Oct 1950, pp. 609–629.

[‡]Department of Defense references may be obtained online at http://stinet.dtic.mil [cited 8 December 2000].